

Calcium phosphate fibers coated with collagen: *In vivo* evaluation of the effects on bone repair

Fabio Roberto Ueno^a, Hueliton Wilian Kido^a, Renata Neves Granito^a,
Paulo Roberto Gabbai-Armelin^a, Angela Maria Paiva Magri^a, Kelly Rosseti Fernandes^a,
Antonio Carlos da Silva^b, Francisco José Correa Braga^b and Ana Claudia Muniz Renno^{a,*}

^a *Department of Biosciences, Federal University of São Paulo (UNIFESP), Santos, SP, Brazil*

^b *Nuclear and Energy Research Institute (IPEN), São Paulo, SP, Brazil*

Received 30 September 2015

Accepted 1 July 2016

Abstract. The aim of this study was to assess the characteristics of the CaP/Col composites, in powder and fiber form, via scanning electron microscopy (SEM), pH and calcium release evaluation after immersion in SBF and to evaluate the performance of these materials on the bone repair process in a tibial bone defect model. For this, four different formulations (CaP powder – CaPp, CaP powder with collagen – CaPp/Col, CaP fibers – CaPf and CaP fibers with collagen – CaPf/Col) were developed. SEM images indicated that both material forms were successfully coated with collagen and that CaPp and CaPf presented HCA precursor crystals on their surface. Although presenting different forms, FTIR analysis indicated that CaPp and CaPf maintained the characteristic peaks for this class of material. Additionally, the calcium assay study demonstrated a higher Ca uptake for CaPp compared to CaPf for up to 5 days. Furthermore, pH measurements revealed that the collagen coating prevented the acidification of the medium, leading to higher pH values for CaPp/Col and CaPf/Col. The histological analysis showed that CaPf/Col demonstrated a higher amount of newly formed bone in the region of the defect and a reduced presence of material. In summary, the results indicated that the fibrous CaP enriched with the organic part (collagen) glassy scaffold presented good degradability and bone-forming properties and also supported Runx2 and RANKL expression. These results show that the present CaP/Col fibrous composite may be used as a bone graft for inducing bone repair.

Keywords: Composite, calcium phosphate, collagen, fibers, bone repair

1. Introduction

Bone tissue engineering (BTE) and the development of synthetic bone grafts have been emerging as a potential alternatives to the use of autologous bone mainly due to their biocompatibility, safety and osteogenic properties [1,2]. One of the crucial points to be considered in BTE is the use of appropriate materials in the construction of tissue-engineered products. Composition and presentation of the material, influence cell adhesion, proliferation and differentiation, determining the success of bone implant [3]. Furthermore, is desirable that synthetic bone grafts chemically, structurally and mechanically mimic natural bone, being constituted by an organic and an inorganic phase [4].

*Corresponding author: Ana Claudia Muniz Renno, Department of Biosciences, Federal University of São Paulo (UNIFESP), Rua Silva Jardim, 136, Santos, SP, Brazil. Tel.: +55 13 38783823; Fax: +55 13 38783825; E-mail: acmr_ft@yahoo.com.br.

In this context, bioceramics, a broad range of inorganic/non-metallic compositions [5], can serve as the inorganic bone phase and include hydroxyapatite, bioactive glasses (BGs) [6,7], such as Biosilicate® [8] and others [9–11]. Similarly, one of the most common material ceramic used is calcium phosphate (CaP). CaP presents excellent osteoconductive properties and can be used in an injectable way, allowing the use of a minimally invasive surgical procedure during clinical use [12,13].

In addition, the incorporation of an organic component into the inorganic phase of the material is strongly desirable to better approximate the bone graft substitute to the structure of bone tissue [4]. In this context, some authors have been introducing collagen to the CaP, which might represent a promising way of improving the biological performance of the material. Collagen is a natural structural protein that cells can attach to and it is bioabsorbable, with a low immunogenicity [4]. Mate-Sanches del Val et al. [14] observed an improved bone contact implant into the bone defect area in femurs of rabbits treated with a porous scaffold manufactured from hydroxyapatite and CaP, enriched with collagen.

Besides the composition, another important point for the success of the graft is the material structure [15]. In BTE, material in powder and porous scaffolds serving as support of tissue formation are commonly used, being able of producing cell adhesion and angiogenesis [16,17]. Although the advantages of these presentations, in most cases, they do not have the ability of acting as fillers for bone defects with irregular shapes [18]. In this context, the possibility of molding a material which can fill bone defects and fractures of different sizes and forms, are a very desirable characteristic required for grafts [19]. These characteristics have been demonstrated by fibrous porous materials [20]. Furthermore, fibrous materials have been demonstrating the ability of stimulating cell attachment and growth, promoting newly bone formation and mineralization [21]. Thus, the obtainment of malleable fibers from bioceramics enriched with collagen seems to be a promising therapeutic approach for using in bone tissue engineering.

With the aim of developing a material able of mimicking bone tissue composition, a composite associating CaP (inorganic part) and collagen (organic part) was manufactured [22] and presented in a fibrous malleable way. It was hypothesized that this bone-like material would present an improved biological performance compared to CaP alone and to the material in powder. Consequently, the present study had 2 aims: first, to assess the biological performance of the introduction of collagen into CaP samples using a tibial bone defect model in rats. Second, to investigate and to compare the effects of CaP and CaP plus collagen in powder (p) and in fibers (f), using the same animal model. To this end, pre-set samples in 4 different formulations (CaP powder: CaPp, CaP powder enriched with collagen: CaPp/Col, CaP fibers: CaPf and CaP fibers enriched with collagen: CaPf/Col) were analyzed via scanning electron microscopy (SEM), pH and calcium release evaluation after immersion. Moreover, the histopathological and immunohistochemistry analysis were performed using a tibial bone defect model in rats.

2. Materials and methods

2.1. Materials

2.1.1. CaP powder (CaPp)

CaP used in this study contained 60.0 wt% of P₂O₅ and 40.0 wt% of CaO, with P₂O₅ (Vetec, 97.0 wt%) and CaO (Nuclear, 95.0 wt%) as precursor compounds. For manufacturing, reactants were mixed in a glass reactor. Initially 500 ml of P₂O₅ (6.0 wt%) solution was deposited in the reactor, followed by the addition of 500 ml of CaO (4.0 wt%) solution. Afterwards, the solution was dried for 7 days, at 60°C and milled to powder grain in an agate mortar (particle sizes of 250 μm). Powder was weighed

and mixed for 30 min in a polyethylene bottle. Premixed batches were melted in a alumina crucible at a temperature of 1500°C (Lindberg Blue vertical super kanthal furnace – USA) [23–25]. The melting time was fixed as 2 h. Samples were quenched in deionized water and milled to powder grain (with sizes ranging from 260–600 µm). No annealing was performed. Samples were cast into a 10 mm × 30 mm cylindrical graphite mold, quenched in deionized water and milled to powder grain (270 µm).

2.1.2. CaP fibers (CaPf)

Fibers were obtained using the same process described above. However, in spite of quenching in water, the melt was quenched in a Hager-Rosengarth apparatus [26,27]. The Hager-Rosengarth process leads the melt to a centrifugal acceleration, leaving the centrifuging disc and cooled in air which is flowing together with the fiber due to this angle speed [28].

2.1.3. Collagen (Col)

Collagen type I (Col I) used in this study was provided by Consulmat (São Carlos, Brazil). Col I from bovine bone was obtained in three main steps: (i) demineralization of bovine cortical bone in chloridric acid (HCl); (ii) dissolution of the cortical bone collagen in 0.5 M acetic acid (C₂H₄O₂) at 40°C and (iii) pH adjustment with ammonium hydroxide (NH₄OH). Granules < 270 µm were obtained.

2.2. Composite preparation

2.2.1. Enrichment of CaP powder with Col (CaPp/Col)

Layers of Collagen and CaP powder were alternately deposited on a substrate (Petri dish) insomuch that the resulting particles were completely coated by Col. Samples were dried during 48 hours in an oven at 40°C and the composite was milled to obtain powder.

2.2.2. Enrichment of CaP fibers with Col (CaPf/Col)

For the fibrous composition enriched with collagen, the collagen solution was homogeneously sprayed on the fibers tappet until it had acquired the wet appearance. Subsequently, the material was dried for 48 h at 40°C.

2.2.3. Preparation of the pre-set composites

Four experimental groups were created: CaPp, CaPp/Col, CaPf and CaPf/Col. All the samples were analyzed using SEM. Before use, the pre-set composites were sterilized by γ -radiation with a minimum dose of 25 kGy (Isotron B.V., Ede, The Netherlands). Before use, the materials were sterilized using a 25 kGy dose of gamma irradiation (IPEN, São Paulo, Brazil).

2.3. Characterization of the composites

2.3.1. Material characterization

Pre-set composites were first examined by SEM observation. The pre-set composites were mounted on aluminum stubs using carbon tape and sputter-coated with gold/palladium prior to examination.

2.3.2. Fourier transform infrared spectroscopy (FT-IR)

FT-IR (Thermo Nicolet Nexus 4000, USA) was performed to evaluate the chemical bonds present in the materials. The examinations were done in the range of 400–1800 cm⁻¹ with a resolution of 2 cm⁻¹. The samples were scanned 128 times for each measurement and the spectrum acquired was the average of all these scans.

2.3.3. Calcium assay

The Ca release/uptake capacity of the materials, CaPp and CaPf, was evaluated according to Kokubo and Takadama [29]. The samples (0.05 g) were placed in glass vials containing 3 mL of Simulated Body Fluid (SBF) at 37°C on a shaker table (70 Hz) for up to 5 days, with refreshment on days 1, 3 and 5. Subsequently to each refreshment, the solution of the previous period was saved for analysis of the calcium content in SBF by the orthocresolphthalein complexone (OCPC) assay [30]. These solutions were incubated overnight in 1 mL of 0.5 N acetic acid on a shaker table. For analysis, 300 µL working reagent was added to 10 µL sample or standard in a 96-well plate. Thereafter, the well plate was incubated for 10 min at room temperature. The absorbance was measured on a microplate spectrophotometer at 570 nm (Molecular Device, SpectraMax M5, Sunnyvale, CA, USA). The standards (between 0 and 100 µg mL⁻¹) were prepared using a CaCl₂ stock solution. Data were acquired from triplicate samples and measured in duplo. The Ca depletion was plotted cumulatively, measuring the difference between the Ca concentration in the sample-free SBF control solutions and the SBF solution in the presence of the different bioactive glass forms.

2.3.4. pH measurements

After each experimental period, the pH of the SBF solutions in contact with the materials was measured ($n = 3$) utilizing a pH electrode (Tecnal T.E.C-51, Piracicaba, Brazil).

2.4. Surgical procedure

Forty young adult male Wistar rats (12 weeks old; weight 295 ± 29 g) were used as experimental animals and randomly distributed into the following groups ($n = 10$): CaPp, CaPp/Col, CaPf and CaPf/Col. The animal experimental plan was reviewed and approved by the Experimental Animal Committee of the Federal University of Sao Paulo (CEUA N 174679) and national guidelines for the care and use of laboratory animals were observed.

Anesthesia was induced and maintained by Isoflurane inhalation (Rhodia Organique Fine Limited). In order to minimize post-operative discomfort, buprenorfine (Temgesic; Reckitt Benckiser Health Care Limited, Schering-Plough, Hoddesdon, UK) was administered intraperitoneally (0.02 mg/kg) directly after the operation and subcutaneously for 2 days after surgery. For inserting implants into the tibial defects, the animals were immobilized on their back and both hind limbs were shaved, washed and disinfected with povidone-iodine. After exposure of the medial compartment of the tibia, a 1.0 mm pilot hole was drilled. The hole was gradually widened until a final defect size of 3 mm in width was reached. Low rotational drill speeds (max. 450 rpm) and constant physiologic saline irrigation were used. After preparation, the defects were thoroughly irrigated and packed with sterile cotton gaze to stop bleeding. Surgery was performed in both legs of the rats and one defect was created in each tibia. The sterilized compositions were placed in the created defect up to its complete filling ($n = 10$ per experimental group). Thereafter, the wound was closed with resorbable Vicryl[®] 5-0 (Johnson & Johnson, St. Stevens-Woluwe, Belgium) after which the skin was closed by staples (Agraven[®]; InstruVet BV, Cuijk, The Netherlands). After 2 weeks of implantation, rats were sacrificed by CO₂ asphyxia. The tibiae were collected for analysis.

2.5. Histological procedures

For the histopathological, morphometrical and immunohistochemical analysis, the tibiae were harvested and fixed in 10% buffer formalin (Merck, Darmstadt, Germany) for 24 hours. They were decalcified

in 10% EDTA (Merck) and embedded in paraffin blocks. Five-micrometer cortical bone slices were obtained with a microtome (Leica Microsystems SP 1600, Nussloch, Germany). The slices were cut perpendicularly to the medial-lateral drilling axis of the implant. At least three non-consecutive sections of each specimen were stained with hematoxylin and eosin (H.E. stain, Merck) and used for analysis.

2.6. Histopathological analysis

Histopathological evaluation was performed under an optical microscope (Olympus, Optical Co. Ltd, Tokyo, Japan). The area of the bone defect was qualitatively evaluated considering the inflammatory process, granulation tissue and newly formed bone. At least three sections of each specimen were examined for each specimen.

2.7. Histomorphometry analysis

Histological sections were quantitatively evaluated via computer-based image analysis techniques (Axiovision 3.0.6 SP4, Carl Zeiss, Jena, Germany). Digitalized images of the defect ($\times 20$) were obtained and the amount of newly formed bone was determined within three regions of interest inside the defect site: ROI1 (upper left border, $1.07 \times 10^6 \mu\text{m}^2$), ROI2 (lower left border, 1.07×10^6), and ROI3 (central region of the right border, 1.07×10^6) [31,32]. The mean tissue area (T.Ar) analyzed was $9.5 \times 10^6 \pm 1.7 \times 10^5 \mu\text{m}^2$. The static indice of bone volume as a percentage of tissue volume (BV/TV, %) was used for the analysis.

2.8. Immunohistochemistry analysis

For the immunohistochemical analysis, xylene was used to remove the paraffin from the serial sections. After this procedure, the sections were rehydrated in graded ethanol and pretreated in a microwave (Electrolux, São Paulo, Brazil) with 0.01 M citric acid buffer (pH 6) for three cycles of 5 min each at 850 W for antigen retrieval. The resulting material was pre-incubated with 0.3% hydrogen peroxide in phosphate-buffered saline (PBS) solution for 5 min in order to inactivate the endogenous peroxidase. Then, the samples were blocked with 5% normal goat serum in PBS for 10 min. The specimens were incubated with anti-Runx2 polyclonal primary antibody (code: sc-8566, Santa Cruz Biotechnology, USA) at a concentration of 1:200, and anti-RANKL polyclonal primary antibody (code: sc-7627, Santa Cruz Biotechnology, USA) also at a concentration of 1:200. Incubation was carried out overnight at 4°C in a refrigerator. This step was followed by two washes in PBS for 10 min. The sections were then incubated with biotin conjugated secondary antibody anti-rabbit IgG (Vector Laboratories, Burlingame, CA, USA) at a concentration of 1:200 in PBS for 1 h. The sections were washed twice with PBS followed by the application of preformed avidin biotin complex conjugated to peroxidase (Vector Laboratories) for 45 min. The bound complexes were visualized by the application of a 0.05% solution of 3-3'-diaminobenzidine solution and counterstained with Harris hematoxylin (Sigma-Aldrich). For control studies of the antibodies, the serial sections were treated with rabbit IgG (Vector Laboratories) at a concentration of 1:200 in place of the primary antibody. Additionally, internal positive controls were performed with each staining bath. Runx2 and RANKL immunoexpressions were evaluated qualitatively in order to assess the presence (or absence) and region of occurrence of the immunomarkers. Three sections of each specimen were examined with a light microscopy (Leica Microsystems AG, Wetzlar, Germany).

2.9. Statistical analysis

Statistical analyses of material degradation and bone formation were performed using SPSS, version 16.0 (SPSS Inc., Chicago, IL, USA). The statistical comparisons were performed using a one-way analysis of variance (ANOVA) with a Tukey multiple comparison post-test. Differences were considered significant at P -values <0.05 .

3. Results

3.1. Material characterization

SEM evaluation of the different materials are depicted in Fig. 1. As expected, CaP particles with diverse sizes could be observed (Fig. 1A and B). Additionally, crystals were observed on the CaP particles (Fig. 1A) and, in regards to CaPp/Col, particles aggregates were observed due to the collagen coating (Fig. 1B). Furthermore, SEM micrographs showed that CaP fibers were successfully obtained from the CaP precursor (Fig. 1C). These fibers were randomly positioned, presenting different diameters (ranging from 500 nm to 1 μ m) (Fig. 1C and D). CaPf, as found for CaPp, also showed crystals on their surface (Fig. 1C). After coating with collagen, the CaPf/Col presented some rougher parts and crystals could not be observed (Fig. 1D).

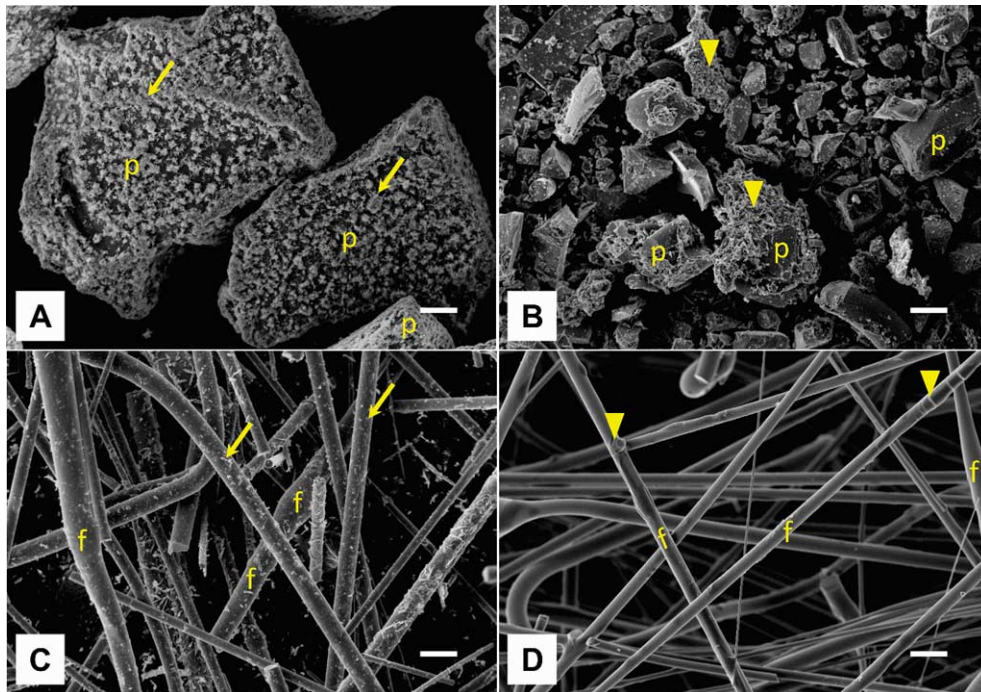


Fig. 1. SEM micrographs of the different materials: CaPp (A); CaPp/Col (B); CaPf (C); CaPf/Col (D). CaP particles (p), CaP fibers (f), crystals (arrows) and collagen (\blacktriangledown). 500 \times magnification. Bars represent 50 μ m.

3.2. Fourier transform infrared spectroscopy (FT-IR)

Figures 2 and 3 show the FT-IR spectra for both forms of CaP. A corresponding P–O link to the CaP amorphous arrangements can be observed. Furthermore, there is indication of chemical bonds associated with asymmetrical PO_4^{3-} in both materials, which also indicates the material amorphous characteristic. On the other hand, there are bonds associated with OH^- groups for both material forms (indicated by “4” and “5” in Figs 2 and 3). This fact is especially clear for the peak at 840 cm^{-1} which appears to be shifted to the right side with wider distribution for the derivative forms.

3.3. Calcium assay

The calcium assay for CaPp and CaPf samples was assessed by measuring quantitatively the calcium concentration as a function of soaking time (Fig. 4). Both forms of the material, presented at day 1 an initial Ca uptake with statistical difference between groups ($p = 0.049$). At day 3, CaPp and CaPf presented some Ca release into the medium, with statistically different Ca values for CaPp ($\sim 119\text{ }\mu\text{g}$) compared to CaPf ($\sim 763\text{ }\mu\text{g}$; $p = 0.0049$). At the last time point, Ca uptake for both groups was noticed, being statistically higher in CaPp ($\sim 2929\text{ }\mu\text{g}$) compared to CaPf ($\sim 972\text{ }\mu\text{g}$; $p = 0.036$).

3.4. pH measurements

Figure 5 demonstrate the pH values for all experimental groups up to 5 days. Similar behaviors were found for CaPp and CaPf, with values ranging between 4.4 and 5.9. Following the same line, similar behaviors were found for CaPp/Col and CaPf/Col, with values ranging between 6.2 and 7.5. Statistical differences for pH values were observed for CaPf/Col compared to CaPp at all time points ($p < 0.05$, Fig. 5). No other difference was observed among groups ($p > 0.05$).

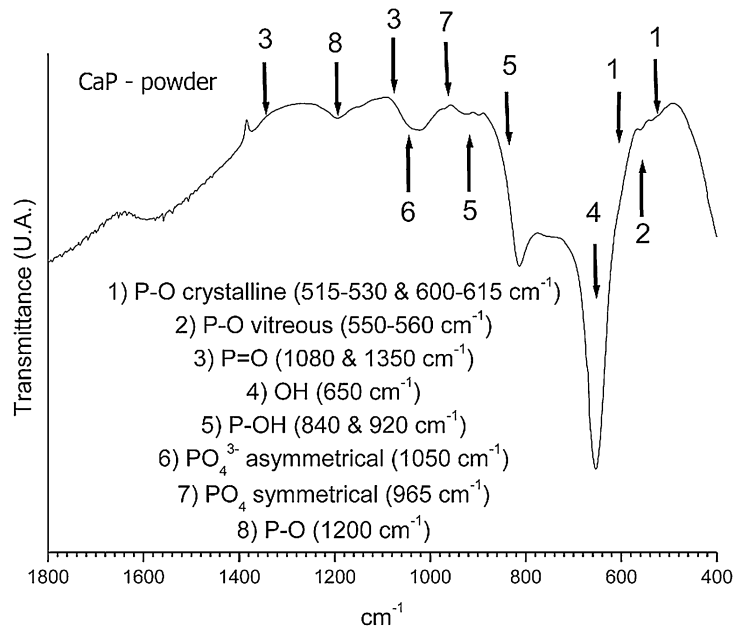


Fig. 2. CaP fine powder ($\leq 270\text{ }\mu\text{m}$) FTIR spectrum.

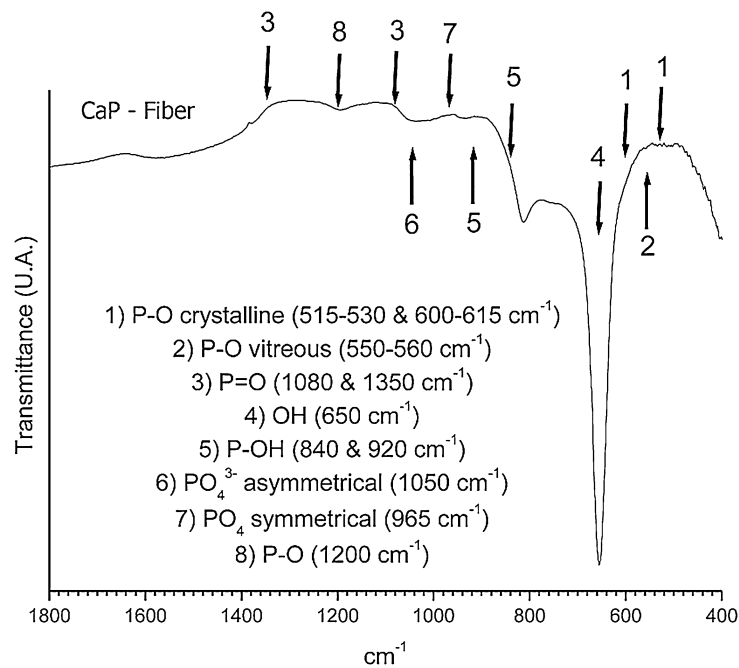
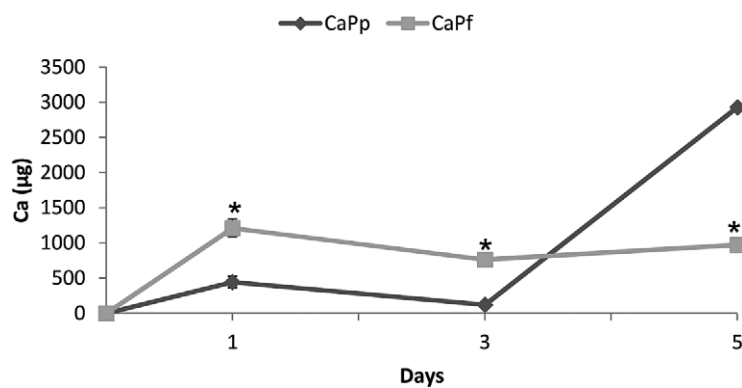


Fig. 3. CaP fibers FTIR spectrum.

Fig. 4. Calcium assay for CaPp and CaPf immersed in SBF for up to 5 days. (*) CaPp compared to CaPf after 1 ($p = 0.049$), 3 ($p = 0.049$) and 5 days ($p = 0.036$) of incubation.

3.5. Histological analysis

Representative histological sections of all experimental groups after 15 days of implantation are depicted in Fig. 6.

In CaPp, it was observed a delimited area of the defect, which was filled with CaP particles of different sizes distributed throughout the defect region (Fig. 6A). In this group, among the CaP particles newly formed bone and granulation tissue was observed (Fig. 6E). In CaPp/Col similar results to the CaPp group were found (Fig. 6F). For CaPf, a reduced amount of material was observed, with granulation tissue and newly formed bone around the material particles and filling the area occupied by the material compared to CaPp and CaPp/Col (Fig. 6G). For CaPf/Col, bone defect was filled mainly with

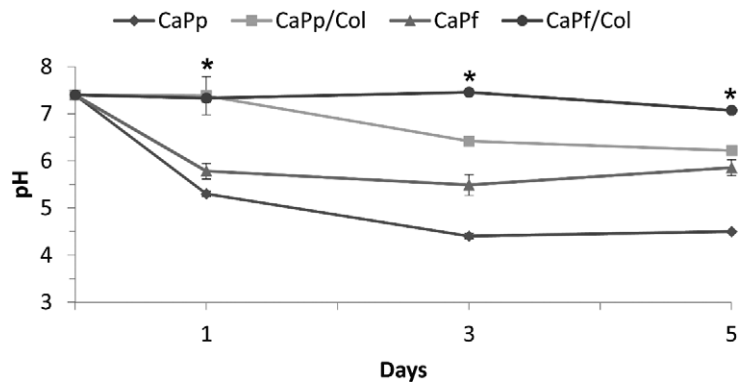


Fig. 5. pH measurements of SBF solution in contact with all compositions for up to 5 days. (*) CaPf/Col compared to CaPp ($p < 0.05$).

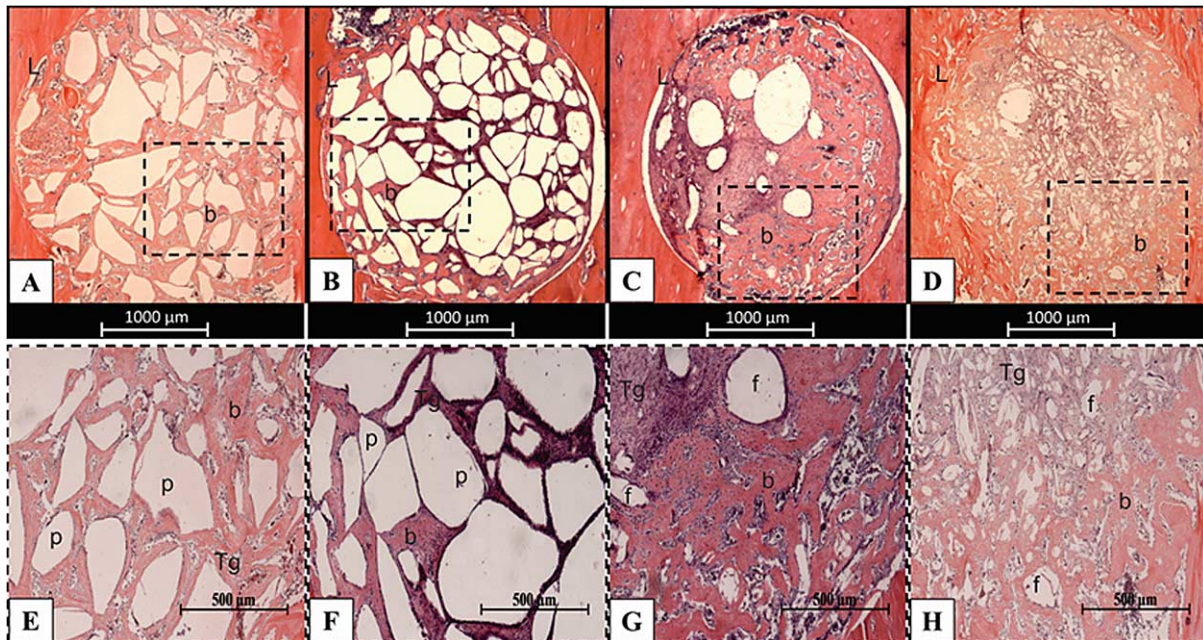


Fig. 6. Histological sections of all groups after 15 days of implantation. CaPp (A), CaPp/Col (B), CaPf (C) and CaPf/Col (D). Newly formed bone (b), defect line (L). Magnification of 2.5 \times . Dashed box indicates the selected region for analysis at a higher magnification of 20 \times . CaPp (E), CaPp/Col (F), CaPf (G), CaPf/Col (H). Newly formed bone (b), powder (p), fibers (f), granulation tissue (Tg). Hematoxylin–Eosin staining.

newly formed bone and granulation tissue. It is possible to observe that, the material fibers were almost completely degraded (Fig. 6D).

3.6. Histomorphometry

Figure 7 demonstrates the means and SE of the newly formed bone of the experimental groups after 15 day of implantation.

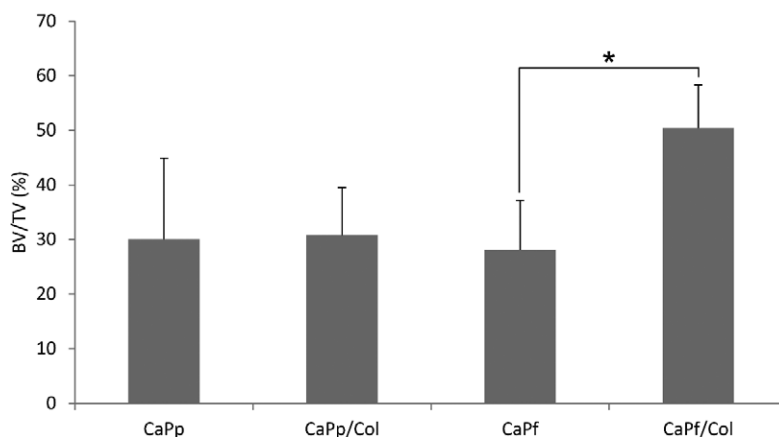


Fig. 7. Bone volume as a percentage of tissue volume. *CaPf/Col compared to CaPf ($p < 0.05$).

The histomorphometry indicated that CaPf/Col presented a significant increase in the amount of newly formed bone compared to CaPf ($p < 0.05$). No other difference was observed among groups ($p > 0.05$, Fig. 7).

3.7. Immunohistochemistry

Runx2 immunoexpression was predominantly detected in the granulation tissue at the edges of the bone defect and around the materials for all groups (Fig. 8). In some samples, osteoblasts cells were also immunomarked for all groups. Similarly to Runx2, RANKL immunoexpression was mainly verified in the granulation tissue at the edges of the bone defect and around the materials for all groups (Fig. 9).

4. Discussion

This work aimed to investigate if the introduction of collagen into CaP samples would present an improved biological performance. Moreover, the present study compared the effects of 2 different material presentation (powder and fibers), via different analysis such as material characterization and biological evaluation by tibial bone implantation. The hypothesis was that the fibrous material would have a more adequate morphology and the incorporation of collagen into this material would present a more appropriate structure toward to attract bone cell growth, facilitating bone formation. SEM images indicated that both material forms were successfully coated with collagen and that CaPp and CaPf presented HCA precursor crystals on their surface. Although presenting different forms, FTIR analysis indicated that CaPp and CaPf maintained the characteristic peaks for this class of material. Additionally, the calcium assay study demonstrated a higher Ca uptake for CaPp compared to CaPf for up to 5 days. Furthermore, pH measurements revealed that the collagen coating prevented the acidification of the medium, leading to higher pH values for CaPp/Col and CaPf/Col. The histological analysis showed that CaPf/Col demonstrated a higher amount of newly formed bone in the region of the defect and a reduced presence of material.

The investigation of the behavior of new biomaterials with osteoconductive properties has been of great interest in orthopedic and dental fields [33–35]. In addition, it is well known that the tissue response to an implanted biomaterial is determined by its composition and morphology [36].

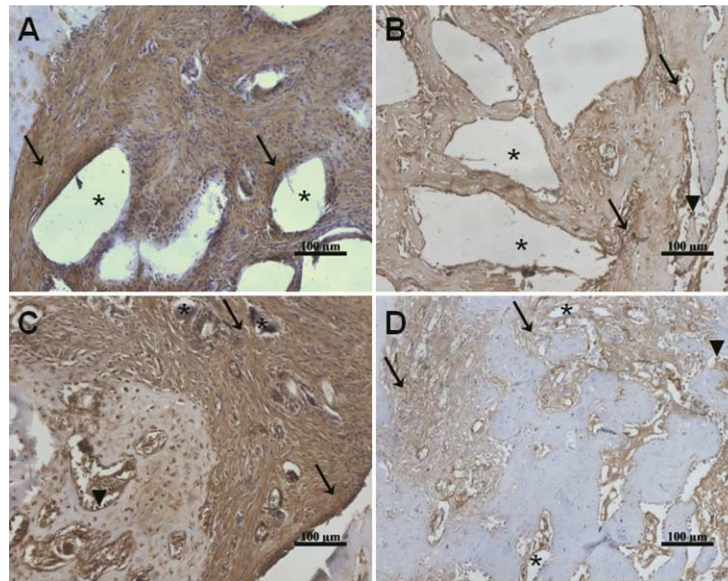


Fig. 8. Representative histological sections of runt-related transcription factor-2 (Runx2) immunohistochemistry. CaPp (A), CaPp/Col (B), CaPf (C) and CaPf/Col (D). Runx2 immunopositivity (arrow), osteoblast (▼) and biomaterial (*).

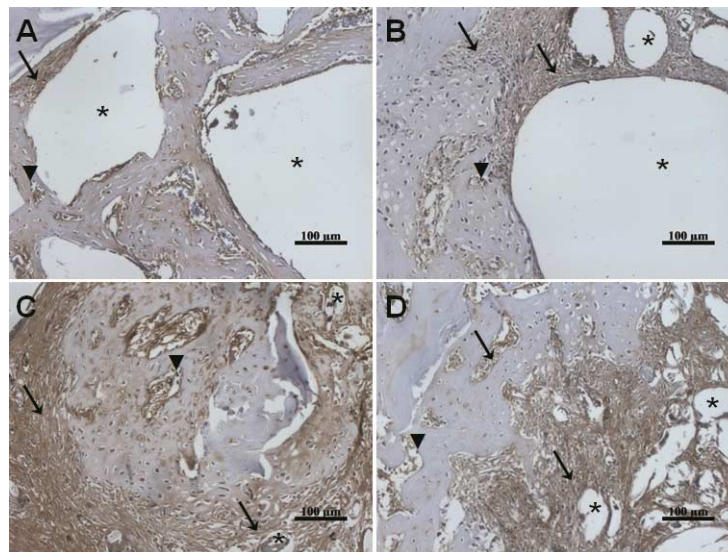


Fig. 9. Representative histological sections of activator of nuclear factor kappa-B ligand (RANKL) immunohistochemistry. CaPp (A), CaPp/Col (B), CaPf (C) and CaPf/Col (D). RANKL immunopositivity (arrow), osteoblast (▼) and biomaterial (*).

The calcium assay showed an increased Ca uptake for CaPp comparing to CaPf for up to 5 days of immersion in SBF. This event may be explained by the irregular (and increased) material surface area presented by CaPp, generating a higher material/solution contact, and, consequently, higher Ca uptake. Accordingly to earlier studies, mineralization preferentially starts within irregular surfaces (i.e. concavities and recesses) rather than on planar surfaces [37].

The pH measurements indicated lower pH values for CaPp and CaPf compared to the materials coated with collagen. This fact is consistent with most of the biomimetic processes, in which are evidenced a pH decrease of the solution during calcium phosphate precipitation [7,38]. In contrast to that, the present work showed that the collagen coating prevented the acidification of the medium, and this event may be pivotal to cell attraction and differentiation toward to the tissue regeneration in the site of injury [39].

Resorption of the bone graft are essential to permit newly formed bone ingrowth [40–42]. As presented in this study, the histological analysis indicate that the introduction of collagen into the fibrous CaP material determine the acceleration of the degradation rate of the material, which substantially stimulate the formation of bone into the defect area. The incorporation of collagen into CaP ceramic matrix may constitute a way of improving biological performance of the bone graft, adding an organic phase of the material [14]. Authors demonstrated that collagen promotes an earlier recruitment and attachment of cells to the biomaterial, allowing bone cell growth and new bone deposition [14,43]. Beside the material composition, the structure of bone substitutes is also important. Fibrous and high porous scaffolds, in general, degrade faster, allowing cell migration, vascularization and tissue ingrowth [44]. Taking all the results together, the association of CaP and collagen would constitute a bone graft with similar characteristics to bone tissue, which may have improved the biological performance of the material. Also, the fibrous structure, associated with the CaP and collagen composite was more beneficial to stimulate bone deposition.

Concerning the immunohistochemistry, it is noteworthy that Runx2 expression was observed in all experimental groups. Runx2 immunofactor stimulates the differentiation of mesenchymal progenitors toward osteoblast cell lineage. Moreover, the upregulation of osteoblastic markers, like osteocalcin, osteopontin and alkaline phosphatase is initiated with Runx2 [45,46]. The presence of this immunomarker for all groups may have influenced osteoblast cell differentiation and consequently, bone formation and deposition. However, a more detailed immunohistochemistry analysis needs to be performed, including quantitative evaluations, to measure the differences among groups. Similarly, RANKL is known as a key factor for differentiation and activation of osteoclasts [47–49]. Pinto et al. [50] determined that bioglass (Biosilicate[®] glass-ceramic) induced a higher RANKL immunoexpression in an experimental bone defects in rats. Similar findings were observed by Kondo et al. [51] who tested b-tricalcium phosphate (b-TCP) using implantation in femoral condyle of rats. In the present study, it may be suggested that the presence of RANKL, in all experimental groups, may have stimulated osteoclast activity, which would have positive effects on bone repair and remodeling.

The results of this initial investigation confirmed the hypothesis that the fibrous composite, coated with collagen, had an accelerated degradation rate and stimulated newly formed bone deposition, constituting a promising alternative to be used as bone grafts for tissue engineering. Future investigations should be performed using different bone defect models such as those of critical-size or compromised situations.

5. Conclusion

In summary, the results indicated that the fibrous CaP enriched with the organic part (collagen) glassy scaffold presented good degradability and bone-forming properties and also supported Runx2 and RANKL expression. Additional studies should be performed to provide more information concerning the late stages of material absorption and bone formation. Further investigations need to be developed to analyze the biological performance of this composite in different situations such as critical bone defects to support the use of this promising fibrous material for bone tissue engineering.

Conflict of interest

The authors have no conflict of interest to report.

References

- [1] D.W. Hutmacher, J.T. Schantz, C.X. Lam, K.C. Tan and T.C. Lim, State of the art and future directions of scaffold-based bone engineering from a biomaterials perspective, *Journal of Tissue Engineering and Regenerative Medicine* **1**(4) (2007), 245–260. doi:[10.1002/term.24](https://doi.org/10.1002/term.24).
- [2] A.R. Amini, C.T. Laurencin and S.P. Nukavarapu, Bone tissue engineering: Recent advances and challenges, *Critical Reviews in Biomedical Engineering* **40**(5) (2012), 363–408. doi:[10.1615/CritRevBiomedEng.v40.i5.10](https://doi.org/10.1615/CritRevBiomedEng.v40.i5.10).
- [3] P. Mesquita, S. Gomes Pde, P. Sampaio, G. Juodzbaly, A. Afonso and M.H. Fernandes, Surface properties and osteoblastic cytocompatibility of two blasted and acid-etched titanium implant systems with distinct microtopography, *Journal of Oral & Maxillofacial Research* **3**(1) (2012), e4.
- [4] Y.S. Pek, S. Gao, M.S. Arshad, K.J. Leck and J.Y. Ying, Porous collagen-apatite nanocomposite foams as bone regeneration scaffolds, *Biomaterials* **29**(32) (2008), 4300–4305. doi:[10.1016/j.biomaterials.2008.07.030](https://doi.org/10.1016/j.biomaterials.2008.07.030).
- [5] L.L. Hench and G. David, Interactions between bioactive glass and collagen: A review and new perspectives, *Journal of The Australian Ceramic Society* **49**(2) (2013), 1–40.
- [6] A.C. Renno, F.C. van de Watering, M.R. Nejadnik, M.C. Crovace, E.D. Zanotto, J.G. Wolke et al., Incorporation of bioactive glass in calcium phosphate cement: An evaluation, *Acta Biomaterialia* **9**(3) (2013), 5728–5739. doi:[10.1016/j.actbio.2012.11.009](https://doi.org/10.1016/j.actbio.2012.11.009).
- [7] A.C.M. Renno, M.R. Nejadnik, F.C.J. van de Watering, M.C. Crovace, E.D. Zanotto, J.P.M. Hoefnagels et al., Incorporation of bioactive glass in calcium phosphate cement: Material characterization and in vitro degradation, *Journal of Biomedical Materials Research Part A* **101A**(8) (2013), 2365–2373. doi:[10.1002/jbm.a.34531](https://doi.org/10.1002/jbm.a.34531).
- [8] R.N. Granito, D.A. Ribeiro, A.C. Renno, C. Ravagnani, P.S. Bossini, O. Peitl-Filho et al., Effects of biosilicate and bioglass 45S5 on tibial bone consolidation on rats: A biomechanical and a histological study, *Journal of Materials Science Materials in Medicine* **20**(12) (2009), 2521–2526. doi:[10.1007/s10856-009-3824-z](https://doi.org/10.1007/s10856-009-3824-z).
- [9] P. Valerio, M.M. Pereira, A.M. Goes and M.F. Leite, The effect of ionic products from bioactive glass dissolution on osteoblast proliferation and collagen production, *Biomaterials* **25**(15) (2004), 2941–2948. doi:[10.1016/j.biomaterials.2003.09.086](https://doi.org/10.1016/j.biomaterials.2003.09.086).
- [10] B. Stevens, Y. Yang, A. Mohandas, B. Stucker and K.T. Nguyen, A review of materials, fabrication methods, and strategies used to enhance bone regeneration in engineered bone tissues, *Journal of Biomedical Materials Research Part B, Applied Biomaterials* **85**(2) (2008), 573–582. doi:[10.1002/jbm.b.30962](https://doi.org/10.1002/jbm.b.30962).
- [11] K.Y. Lee, M. Park, H.M. Kim, Y.J. Lim, H.J. Chun, H. Kim et al., Ceramic bioactivity: Progresses, challenges and perspectives, *Biomedical Materials* **1**(2) (2006), R31–R37. doi:[10.1088/1748-6041/1/2/R01](https://doi.org/10.1088/1748-6041/1/2/R01).
- [12] W.J. Habraken, J.G. Wolke, A.G. Mikos and J.A. Jansen, Injectable PLGA microsphere/calcium phosphate cements: Physical properties and degradation characteristics, *Journal of Biomaterials Science Polymer Edition* **17**(9) (2006), 1057–1074. doi:[10.1163/156856206778366004](https://doi.org/10.1163/156856206778366004).
- [13] E.W. Bodde, W.J. Habraken, A.G. Mikos, P.H. Spauwen and J.A. Jansen, Effect of polymer molecular weight on the bone biological activity of biodegradable polymer/calcium phosphate cement composites, *Tissue Engineering Part A* **15**(10) (2009), 3183–3191. doi:[10.1089/ten.tea.2008.0694](https://doi.org/10.1089/ten.tea.2008.0694).
- [14] J.E. Maté Sánchez de Val, J.L. Calvo Guirado, M.P. Ramírez Fernández, R.A. Delgado Ruiz, P. Mazón and P.N. De Aza, In vivo behavior of hydroxyapatite/ β -TCP/collagen scaffold in animal model. Histological, histomorphometrical, radiological, and SEM analysis at 15, 30, and 60 days, *Clinical Oral Implants Research* (2015), to appear. doi:[10.1111/clr.12656](https://doi.org/10.1111/clr.12656).
- [15] B. Marelli, C.E. Ghezzi, D. Mohn, W.J. Stark, J.E. Barralet, A.R. Boccaccini et al., Accelerated mineralization of dense collagen-nano bioactive glass hybrid gels increases scaffold stiffness and regulates osteoblastic function, *Biomaterials* **32**(34) (2011), 8915–8926. doi:[10.1016/j.biomaterials.2011.08.016](https://doi.org/10.1016/j.biomaterials.2011.08.016).
- [16] M. Mastrogiacomo, S. Scaglione, R. Martinetti, L. Dolcini, F. Beltrame, R. Cancedda et al., Role of scaffold internal structure on in vivo bone formation in macroporous calcium phosphate bioceramics, *Biomaterials* **27**(17) (2006), 3230–3237. doi:[10.1016/j.biomaterials.2006.01.031](https://doi.org/10.1016/j.biomaterials.2006.01.031).
- [17] M. Spector, Biomaterials-based tissue engineering and regenerative medicine solutions to musculoskeletal problems, *Swiss Medical Weekly* **136**(19–20) (2006), 293–301.
- [18] C. Wu, Y. Zhu, J. Chang, Y. Zhang and Y. Xiao, Bioactive inorganic-materials/alginate composite microspheres with controllable drug-delivery ability, *Journal of Biomedical Materials Research Part B, Applied Biomaterials* **94**(1) (2010), 32–43.

- [19] A.R. Boccaccini and V. Maquet, Bioresorbable and bioactive polymer/bioglass[®] composites with tailored pore structure for tissue engineering applications, *Composites Science and Technology* **63**(16) (2003), 2417–2429. doi:10.1016/S0266-3538(03)00275-6.
- [20] N. Sachot, O. Castano, M.A. Mateos-Timoneda, E. Engel and J.A. Planell, Hierarchically engineered fibrous scaffolds for bone regeneration, *Journal of the Royal Society, Interface/The Royal Society* **10**(88) (2013), 20130684. doi:10.1098/rsif.2013.0684.
- [21] E.I. Pascu, J. Stokes and G.B. McGuinness, Electrospun composites of PHBV, silk fibroin and nano-hydroxyapatite for bone tissue engineering, *Materials Science & Engineering C, Materials for Biological Applications* **33**(8) (2013), 4905–4916. doi:10.1016/j.msec.2013.08.012.
- [22] M.T. Souza, E.D. Zanotto and O. Peitl-Filho, Inventor Vitreous composition, bioactive glassy fibers and tissues. Patent Application No. BR 10 2013 020961 9. Universidade Federal de São Carlos, Brazil, 2013.
- [23] A. Brangule and K.A. Gross, Importance of FTIR spectra deconvolution for the analysis of amorphous calcium phosphates, *Materials Science and Engineering* **77** (2015), 012027.
- [24] E. Beniash, R.A. Metzler, R.S. Lam and P.U. Gilbert, Transient amorphous calcium phosphate in forming enamel, *Journal of Structural Biology* **166**(2) (2009), 133–143. doi:10.1016/j.jsb.2009.02.001.
- [25] A.C. Silva, A.H. Aparecida and F.J.C. Braga, Dispersed hydroxyapatite Bioglass 45S5 composites: Comparative evaluation of the use of bovine bone and synthetic hydroxyapatite, *Materials Science Forum* **727** (2012), 1147–1152. doi:10.4028/www.scientific.net/MSF.727-728.1147.
- [26] R. Friedrich and H. Fritz, Apparatus and method for production of fibers from glass, slag, and the like meltable materials. Google Patents; 1941.
- [27] F. Braga, A.C. Silva, S. Allegrini Jr. and C. Otoni (eds), Calcium phosphate graft substitute: When the impact of innovation is in the form rather than content, in: *26th Annual Conference of the European Society of Biomaterials*, Liverpool, 2014.
- [28] J.M.F. Navarro, El Vidrio. Madrid: Consejo Superior de Invest. Científicas – Fundación Centro Nacional del Vidrio, 2003.
- [29] T. Kokubo and H. Takadama, How useful is SBF in predicting in vivo bone bioactivity?, *Biomaterials* **27**(15) (2006), 2907–2915. doi:10.1016/j.biomaterials.2006.01.017.
- [30] R.E. Mooren, E.J. Hendriks, J.J. van den Beucken, M.A. Merckx, G.J. Meijer, J.A. Jansen et al., The effect of platelet-rich plasma in vitro on primary cells: Rat osteoblast-like cells and human endothelial cells, *Tissue Engineering Part A* **16**(10) (2010), 3159–3172. doi:10.1089/ten.tea.2009.0832.
- [31] P. Oliveira, D.A. Ribeiro, E.F. Pipi, P. Driusso, N.A. Parizotto and A.C. Renno, Low level laser therapy does not modulate the outcomes of a highly bioactive glass-ceramic (Biosilicate) on bone consolidation in rats, *Journal of Materials Science Materials in Medicine* **21**(4) (2010), 1379–1384. doi:10.1007/s10856-009-3945-4.
- [32] R.N. Granito, A.C. Renno, C. Ravagnani, P.S. Bossini, D. Mochiuti, V. Jorgetti et al., In vivo biological performance of a novel highly bioactive glass-ceramic (Biosilicate[®]): A biomechanical and histomorphometric study in rat tibial defects, *Journal of Biomedical Materials Research Part B, Applied Biomaterials* **97**(1) (2011), 139–147. doi:10.1002/jbm.b.31795.
- [33] L.L. Hench and J.M. Polak, Third-generation biomedical materials, *Science* **295**(5557) (2002), 1014–1017.
- [34] O. Gauthier, R. Muller, D. von Stechow, B. Lamy, P. Weiss, J.M. Bouler et al., In vivo bone regeneration with injectable calcium phosphate biomaterial: A three-dimensional micro-computed tomographic, biomechanical and SEM study, *Biomaterials* **26**(27) (2005), 5444–5453. doi:10.1016/j.biomaterials.2005.01.072.
- [35] D.P. Link, J. van den Dolder, J.J. van den Beucken, V.M. Cuijpers, J.G. Wolke, A.G. Mikos et al., Evaluation of the biocompatibility of calcium phosphate cement/PLGA microparticle composites, *Journal of Biomedical Materials Research Part A* **87**(3) (2008), 760–769. doi:10.1002/jbm.a.31831.
- [36] D.L. Wise, D.J. Trantolo, D.E. Altobelli, M.J. Yaszemski, J.D. Gresser and E.R. Schwartz, *Encyclopedic Handbook of Biomaterials and Bioengineering. Part B: Applications*, Marcel Dekker, Inc., New York, 1995.
- [37] E.R. Urquia Edreira, J.G. Wolke, J.A. Jansen and J.J. van den Beucken, Influence of ceramic disk material, surface hemispheres, and SBF volume on in vitro mineralization, *Journal of Biomedical Materials Research Part A* **103**(8) (2015), 2740–2746. doi:10.1002/jbm.a.35406.
- [38] G.P. Dominique, *Biomechanics and Biomaterials in Orthopedics*, Springer-Verlag, London, 2004.
- [39] A.C. Taylor, Responses of cells to pH changes in the medium, *The Journal of Cell Biology* **15** (1962), 201–209. doi:10.1083/jcb.15.2.201.
- [40] P. Ruhé, E. Hedberg, N.T. Padron, P. Spauwen, J. Jansen and A. Mikos, Biocompatibility and degradation of poly(DL-lactide-co-glycolic acid)/calcium phosphate cement composites, *J. Biomed. Mater. Res. A* **74A**(4) (2005), 533–544. doi:10.1002/jbm.a.30341.
- [41] X. Qi, J. Ye and Y. Wang, Improved injectability and in vitro degradation of a calcium phosphate cement containing poly(lactide-co-glycolide) microspheres, *Acta Biomater.* **4**(6) (2008), 1837–1845. doi:10.1016/j.actbio.2008.05.009.

- [42] F.C.J. van de Watering, J.J.J.P. van den Beucken, X.F. Walboomers and J.A. Jansen, Calcium phosphate/poly(d,l-lactic-co-glycolic acid) composite bone substitute materials: Evaluation of temporal degradation and bone ingrowth in a rat critical-sized cranial defect, *Clin. Oral. Implants Res.* **23**(2) (2012), 151–159. doi:[10.1111/j.1600-0501.2011.02218.x](https://doi.org/10.1111/j.1600-0501.2011.02218.x).
- [43] Z.Q. Zhou, D.P. Ye, W.G. Liang, B. Wang and Z.Z. Zhu, Preparation and characterization of a novel injectable strontium-containing calcium phosphate cement with collagen, *Chinese Journal of Traumatology (Zhonghua chuang shang za zhi/Chinese Medical Association)* **18**(1) (2015), 33–38.
- [44] P.R. Gabbai-Armelin, M.T. Souza, H.W. Kido, C.R. Tim, P.S. Bossini, A.M. Magri et al., Effect of a new bioactive fibrous glassy scaffold on bone repair, *Journal of Materials Science Materials in Medicine* **26**(5) (2015), 177. doi:[10.1007/s10856-015-5516-1](https://doi.org/10.1007/s10856-015-5516-1).
- [45] F. Afzal, J. Polak and L. Buttery, Endothelial nitric oxide synthase in the control of osteoblastic mineralizing activity and bone integrity, *The Journal of Pathology* **202**(4) (2004), 503–510. doi:[10.1002/path.1536](https://doi.org/10.1002/path.1536).
- [46] X. Zhang, E.M. Schwarz, D.A. Young, J.E. Puzas, R.N. Rosier and R.J. O’Keefe, Cyclooxygenase-2 regulates mesenchymal cell differentiation into the osteoblast lineage and is critically involved in bone repair, *The Journal of Clinical Investigation* **109**(11) (2002), 1405–1415. doi:[10.1172/JCI0215681](https://doi.org/10.1172/JCI0215681).
- [47] V. Lemaire, F.L. Tobin, L.D. Groller, C.R. Cho and L.J. Suva, Modeling the interactions between osteoblast and osteoclast activities in bone remodeling, *Journal of Theoretical Biology* **229**(3) (2004), 293–309. doi:[10.1016/j.jtbi.2004.03.023](https://doi.org/10.1016/j.jtbi.2004.03.023).
- [48] A.E. Kearns, S. Khosla and P.J. Kostenuik, Receptor activator of nuclear factor kappaB ligand and osteoprotegerin regulation of bone remodeling in health and disease, *Endocrine Reviews* **29**(2) (2008), 155–192. doi:[10.1210/er.2007-0014](https://doi.org/10.1210/er.2007-0014).
- [49] A.P. Anandarajah, Role of RANKL in bone diseases, *Trends in Endocrinology and Metabolism: TEM* **20**(2) (2009), 88–94. doi:[10.1016/j.tem.2008.10.007](https://doi.org/10.1016/j.tem.2008.10.007).
- [50] K.N. Pinto, C.R. Tim, M.C. Crovace, M.A. Matsumoto, N.A. Parizotto, E.D. Zanotto et al., Effects of biosilicate® scaffolds and low-level laser therapy on the process of bone healing, *Photomedicine and Laser Surgery* **31**(6) (2013), 252–260. doi:[10.1089/pho.2012.3435](https://doi.org/10.1089/pho.2012.3435).
- [51] N. Kondo, A. Ogose, K. Tokunaga, T. Ito, K. Arai, N. Kudo et al., Bone formation and resorption of highly purified beta-tricalcium phosphate in the rat femoral condyle, *Biomaterials* **26**(28) (2005), 5600–5608. doi:[10.1016/j.biomaterials.2005.02.026](https://doi.org/10.1016/j.biomaterials.2005.02.026).

Copyright of Bio-Medical Materials & Engineering is the property of IOS Press and its content may not be copied or emailed to multiple sites or posted to a listserv without the copyright holder's express written permission. However, users may print, download, or email articles for individual use.